

Mateusz NIEDŹWIEDŹ*, Marek BARA**, Joanna Korzekwa***, Sławomir KAPTACZ****, Maciej SOWA*****, Aleksander OLESIŃSKI*****, Wojciech SIMKA*****

INFLUENCE OF PLASMA ELECTROLYTIC OXIDATION PARAMETERS ON TRIBOLOGICAL PROPERTIES OF LAYERS PRODUCED ON AZ31B MAGNESIUM ALLOY

WPLYW PARAMETRÓW PLAZMOWEGO UTLENIANIA ELEKTROLITYCZNEGO NA WŁAŚCIWOŚCI TRIBOLOGICZNE WARSTW WYTWORZONYCH NA STOPIE MAGNEZU AZ31B

Key words: plasma electrolytic oxidation, oxide layers, magnesium alloys, tribology.

Abstract: The article discusses the effect of Plasma Electrolytic Oxidation (PEO) on the tribological properties of oxide layers produced on the AZ31B magnesium alloy. The layers were formed using PEO (AC+DC) in an alkaline electrolyte with a current density of 10 A/dm². The oxidation parameters (process time, cathodic voltage) were selected based on a research plan. The tribological properties of the samples were tested on a T-17 tester in a pin-on-plate test under technically dry friction conditions, using a pin made of PEEK-HPV polymer. The tests allowed the determination of the coefficient of friction, linear wear, and changes in the mass of the sample and pin. Profilometric measurements were also made before and after the friction process. An increase in the oxidation time and cathodic voltage led to an increase in the thickness and roughness of the oxide layer. The sample oxidized under the highest parameters exhibited the greatest thickness, as well as the highest amplitude and Abbott–Firestone bearing ratio parameters. It was found that with increasing process time and cathodic voltage, the coefficient of friction (μ) and polymer pin wear increased. Sample C, which had the highest processing parameters, showed the best tribological properties, with a coefficient of friction of 0.253 and a linear wear of 0.057 mm. Due to friction, a significant amount of opaque tribofilm was deposited on sample C, resulting in the highest mass wear of the pin (5.33 mg) and an increase in the mass of the sample by 0.74 mg.

Słowa kluczowe: plazmowe utlenianie elektrolityczne, warstwy tlenkowe, stopy magnezu, tribologia.

Streszczenie: W artykule omówiono wpływ plazmowego utleniania elektrolitycznego (PEO) na tribologiczne właściwości warstw tlenkowych wytworzonych na stopie magnezu AZ31B. Warstwy utleniono przy użyciu PEO (AC+DC) w zasadowym elektrolicie, z gęstością prądową 10 A/dm². Parametry utleniania (czas procesu, napięcie katodowania) były dobierane na podstawie planu badawczego. Właściwości tribologiczne próbek zbadano na testerze T-17 w teście trzpień- płytkę, w warunkach tarcia technicznie suchego wykorzystując trzpień wykonany z tworzywa PEEK-HPV. Testy pozwoliły na określenie współczynnika tarcia, zużycia liniowego oraz zmiany masy próbki i trzpienia. Wykonano także pomiary profilografometryczne przed i po procesie tarcia. Wzrost czasu utleniania i napięcia katodowania wpływa na wzrost grubości i chropowatości warstwy tlenkowej. Próbkę utlenianą w najwyższych parametrach charakteryzowała się najwyższą grubością oraz najwyższymi parametrami amplitudowymi i krzywej nośności Abotta–Firestone. Stwierdzono, że wraz ze wzrostem czasu procesu i napięcia katodowania zwiększa się współczynnik tarcia μ oraz zużycie polimerowego trzpienia. Próbka C charakteryzująca się najwyższymi parametrami procesu wytwarzania cechowała się najwyższymi parametrami tribologicznymi. Współczynnik tarcia μ wyniósł: 0,253, a zużycie liniowe trzpienia: 0,057 mm. W wyniku tarcia na warstwie próbki C osadziła się znaczna ilość nieprzezroczystego filmu ślizgowego, co wynikało także z największego zużycia masowego trzpienia (5,33 mg) oraz wzrostu masy próbki o 0,74 mg.

* ORCID: 0000-0001-9279-3121. University of Silesia in Katowice, Faculty of Science and Technology, Institute of Materials Engineering, 75 Pułku Piechoty 1a, 41-500 Chorzów, Poland, e-mail: mateusz.niedzwiedz@us.edu.pl.

** ORCID: 0000-0002-3488-759X. University of Silesia in Katowice, Faculty of Science and Technology, Institute of Materials Engineering, 75 Pułku Piechoty 1a, 41-500 Chorzów, Poland, marek.bara@us.edu.pl.

*** ORCID: 0000-0002-3289-4526. University of Silesia in Katowice, Faculty of Science and Technology, Institute of Materials Engineering, 75 Pułku Piechoty 1a, 41-500 Chorzów, Poland, e-mail: joanna.korzekwa@us.edu.pl.

**** ORCID: 0000-0002-0584-8655. University of Silesia in Katowice, Faculty of Science and Technology, Institute of Materials Engineering, 75 Pułku Piechoty 1a, 41-500 Chorzów, Poland, e-mail: slawomir.kaptacz@us.edu.pl.

***** ORCID: 0000-0002-5783-9240. Silesian University of Technology, Faculty of Chemistry, Akademicka 2A Str., 44-100 Gliwice, Poland, e-mail: maciej.sowa@polsl.pl.

***** Silesian University of Technology, Faculty of Chemistry, Akademicka 2A Str., 44-100 Gliwice, Poland.

***** ORCID: 0000-0002-2648-5523. Silesian University of Technology, Faculty of Chemistry, Akademicka 2A Str., 44-100 Gliwice, Poland, e-mail: wojciech.simka@polsl.pl.

INTRODUCTION

The formation of oxide layers on magnesium alloys is an extremely important process in the field of tribology [L. 1]. One of the frequently used advanced techniques is plasma oxidation, which allows for the formation of hard and durable protective layers on the surface of the magnesium alloy [L. 2]. Magnesium alloys, including the AZ31B alloy, are commonly used in many industrial fields due to their lightness and strength [L. 3, 4]. The plasma oxidation process consists in irradiating the surface of a magnesium alloy with plasma, which is an ionized gas with high temperatures. This leads to chemical reactions between the metal surface and gas particles, such as oxygen, forming magnesium oxides with different properties [L. 5]. In contrast to the classic plasma oxidation, plasma electrolytic oxidation (PEO) is an environmentally friendly, electrochemical method of surface modification, which, similarly to conventional anodizing [L. 6], allows to obtain an oxide layer on the metal surface, which protects the metal alloy against weather conditions, aggressive chemicals and other harmful factors [L. 7]. Oxide layers obtained by plasma electrolytic oxidation have many advantages. First of all, they improve corrosion resistance [L. 8], but also increase durability and hardness, extending the life of the surface of magnesium alloys [L. 9]. In addition, these layers can also improve the tribological properties of the material, such as reducing friction forces, abrasion and wear [L. 10]. The use of plasma electrolytic oxidation to form oxide layers on magnesium alloys is widely used in various fields, such as the aerospace, automotive, electronics and medical industries [L. 11–13]. Thanks to this technology, it is possible to increase the durability and performance of magnesium alloys in demanding operating conditions. This process is a significant step forward compared to conventional anodizing, contributing to the development and expansion of the applications of these materials. It gives the opportunity to use the lightness and strength of magnesium alloys to an even greater extent, while ensuring protection against corrosion and improving tribological properties. The formation of oxide layers by plasma oxidation has many advantages. Thanks to the plasma oxidation technology and the formation of oxide layers, the AZ31B magnesium alloy can be effectively protected against corrosion and show better tribological properties, which translates

into its use in a wide range of fields. The aim of the manuscript was to determine the influence of plasma electrolytic oxidation parameters (process time, cathodization voltage) on the tribological properties of layers produced on the AZ31B magnesium alloy.

MATERIALS AND METHODS

Research material

The research material consisted of oxide layers produced on a magnesium alloy with the trade name AZ31B and the magnesium alloy itself without modifications, used as a reference sample. The magnesium alloy with aluminum, zinc and manganese used in the tests is characterized by low density, which allows for its wide use in light engineering structures. In addition, thanks to the high content of magnesium and aluminum, it is highly susceptible to oxidation.

The samples were cut from 5 mm thick sheet metal and their target dimensions for oxidation were: 62.5 mm x 16 mm x 5 mm. The preparation of the samples consisted in grinding on a polisher with the use of water SiC abrasive paper with a gradation of 240 at a rotational speed of 150 rpm. The aim of such treatment was to quickly and mechanically remove impurities from the sample surface and give it the same condition before each process. In the next step, to degrease the samples, they were placed in an ultrasonic cleaner for 5 minutes, using isopropyl alcohol as the working medium. Sample preparation was completed by thorough rinsing in distilled water and leaving to dry.

The layers were produced using AC+DC plasma electrolytic oxidation with a trapezoidal voltage waveform, using a KIKUSUI PCR2000WEA power supply. In positive current cycles, the magnesium alloy sample was the anode, the cathode was made of stainless steel. A constant current density of 10 A/dm² was used and the pulse frequency was set to 50 Hz for all layers. In the positive current cycles, the voltage limit was set at 400 V, while the maximum voltage values in the negative cycles, along with the process times, were selected on the basis of a bivariate research plan and are presented in **Table 1**. The plasma electrolytic oxidation process was carried out in a two-component electrolyte consisting of an aqueous solution of sodium metasilicate (Na₂SiO₃) 5 g/L and sodium hydroxide (NaOH) 5 g/L. The temperature of the

electrolyte was stabilized with a cryostat and was $303\pm 5\text{K}$, the electrolyte was additionally stirred with a pump.

During the tribological tests, a PEEK-HPV pin was used as a tribo partner. The material consists of polyetheretherketone reinforced with carbon fibres, graphite lubricants and PTFE. The additives provide the material with excellent wear resistance, a low coefficient of friction and the best machinability of all PEEK polymers. The material is additionally characterized by high mechanical strength and stiffness. These properties allow for a wide range of applications, e.g. as wear guides, bearings, bushings, rollers, but also for valves and seals.

Table 1. List of oxidation parameters on a natural and normal scale for oxide layers

Tabela 1. Zestawienie parametrów utleniania w skali naturalnej oraz unormowanej dla warstw tlenkowych

Sample	Controlled factors			
	On a natural scale		On a standard scale	
	Cathode Voltage [V]	Process Time [min]	x1	x2
A	20	30	1	-1
B	5	60	-1	1
C	20	60	1	1
D	5	30	-1	-1

Research methodology

Measurements of the average thickness of the oxide layer were made using the Fischer Dualscope MP40 contact meter, whose operating methodology is based on the principle of eddy currents. Twenty measurements were made on the entire surface of the layer for each sample. The measurements allowed to calculate the average thickness of the layers along with standard deviations.

Tribological tests were performed with the use of the T-17 tester for the pin-plate friction junction, using technically dry friction, in reciprocating motion. During the tribological runs on the 15 km road, a constant unit load of 0.5 MPa and a constant average sliding speed of 0.2 m/s were used. The tests were carried out at a strictly defined ambient temperature of $298 \pm 1\text{K}$ and air humidity of $40 \pm 10\%$. The friction force values were measured using the Spider 8 transducer and the data was exported to a computer. Then, the results were

saved using the Catman 4.5 software and used for calculations. The coefficient of friction for each sample was calculated from a stabilized range of friction force values. Using the WIT3 displacement measurement sensor, the linear wear of the pin was measured. Using the weight method, the average weight change of the sample and the mass wear of the pin were measured. Tests were performed with one replicate for all samples.

Profilographometric tests were carried out before and after the friction process for both layers and pins constituting a tribo partner. Form TalySurf Series 2 50i contact profilographometer (Taylor Hobson Ltd., Leicester, UK) was used for the measurements. The measurements were made in accordance with the EN ISO 4287 standard (replaced with EN ISO 21920 in 2022), using a sampling length $\lambda_c = l_r = 5\text{ mm}$ and an evaluation length $l_n = 0.8\text{ mm}$. The analysis was carried out on 5 profiles of the samples (before and after the friction process). The fragment for visualization has been cut out from the central part of the profile. Based on the measurements, the amplitude parameters of the surface were determined, along with the parameters of the load-bearing curves and the surface roughness profiles.

Tests were carried out using a scanning electron microscope (SEM) on the surface of the samples, which allowed the observation of the applied sliding film after the tribological test. A magnification of 500x was used, which enabled the determination of the degree of application of the sliding film on the oxide layer and the magnesium alloy.

RESULTS AND DISCUSSION

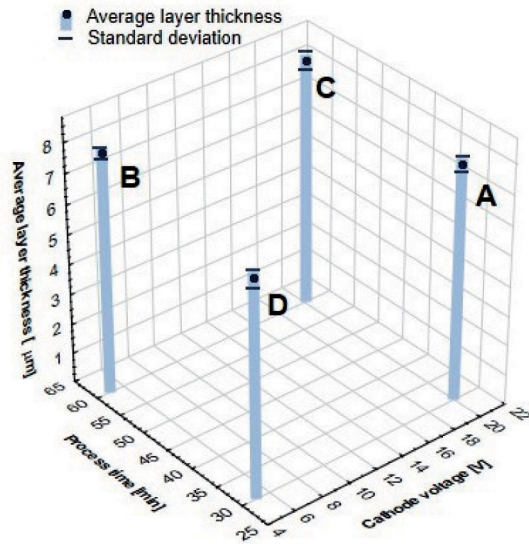
Table 2 presents the average measurements of the thickness of the oxide layers along with standard deviations. Differences in the thickness of individual layers result from different parameters of plasma electrolytic oxidation. The greatest thickness of the oxide layer was measured for sample C ($8.32\text{ }\mu\text{m}$) produced at the highest cathodic voltage (20 V) and the longest process time (60 min). The smallest layer thickness was measured for sample D produced at the lowest cathodic current (5 V) and the shortest time of 30 minutes. It can be concluded that the highest values of the cathodic voltage and the longest process times influence the formation of the thickest layers, while the thinnest layers are formed at the shortest times and the lowest cathodic voltages.

Table 2. List of average layer thickness measurements

Tabela 2. Zestawienie średnich pomiarów grubości warstw

Sample	Average Layer Thickness [μm]	Standard Deviation [μm]
A	7.88	0.25
B	7.99	0.18
C	8.32	0.31
D	7.19	0.27

In order to visualize the influence of the cathodic voltage and time of the plasma electrolytic oxidation process on the thickness of the oxide layer, a graph of dependence was made (**Fig. 1**). Analyzing the influence of the cathodic voltage during the oxidation process and the oxidation time, one can see their significant effect on the increase in the thickness of the oxide layer. The process is carried out using a complex anode-cathode cycle to prevent the intensification of plasma microdischarges on the surface, which occurs during DC operation. Suppression of too strong discharges can be achieved by conducting the process in the unipolar impulse mode (only anode). However, it is worth noting that the oxide/hydroxide layer that forms has the characteristics of a dielectric material, which leads to the generation of a strong charging current for the resulting capacitor, thereby degrading the energy efficiency of the process. During the cathode cycle of the process, part of the current is used to discharge the positive voltage accumulated in the anode cycle [L. 14]. There is also the evolution of hydrogen, which plays an important role in shaping the microstructure of the layers and its electrical properties, which is essential in the energy context of the process and the properties of the obtained layers [L. 15, 16].

**Fig. 1. Dependence of the thickness of the oxide layer on the cathodic voltage and process time**

Rys. 1. Zależność grubości warstwy tlenkowej od napięcia katodowania i czasu procesu

Tribological tests of samples (magnesium alloy and oxide layers) with PEEK-HPV material allowed to determine the coefficient of friction μ and linear wear of the pin (**Table 3**). The highest coefficient of friction μ was determined for sample C (0.253), whose layer was formed during oxidation in the longest time (60 minutes) and at the highest cathodic voltage (20 V). This sample is also characterized by the greatest thickness. The lowest coefficient of friction μ (0.235) was characterized by a magnesium alloy sample that was not modified by plasma electrolytic oxidation. The highest linear wear of the pin (0.0637 mm) was also determined for it, while the lowest (0.0485 mm) was determined for sample D with the lowest coefficient of friction μ among the oxide layers.

Table 3. Mean values of coefficient of friction and linear wear of the pinTabela 3. Średnie wartości współczynnika tarcia μ oraz zużycia liniowego trzpienia

Sample	Average Coefficient of Friction μ	Standard Deviation	Linear Wear of the Pin [mm]	Standard Deviation [mm]
A	0.242	0.006	0.049	0.003
B	0.251	0.002	0.052	0.005
C	0.253	0.002	0.057	0.004
D	0.236	0.003	0.048	0.007
Mg	0.235	0.005	0.064	0.006

Based on the determined coefficients of friction μ and linear wear of the PEEK-HPV pin, graphs were made (Fig. 2) to visualize the dependence on the manufacturing parameters. From the analysis of the graphs of the dependence of the friction coefficient μ on the layer production parameters it followed that the increase in both the

process time and the cathodic voltage increases the coefficient of friction μ (Fig. 2a). A similar relationship can be found between the production parameters and the linear wear of the polymer pin (Fig. 2b), which proves the proportionality of the coefficient of friction μ to the linear wear of the pin.

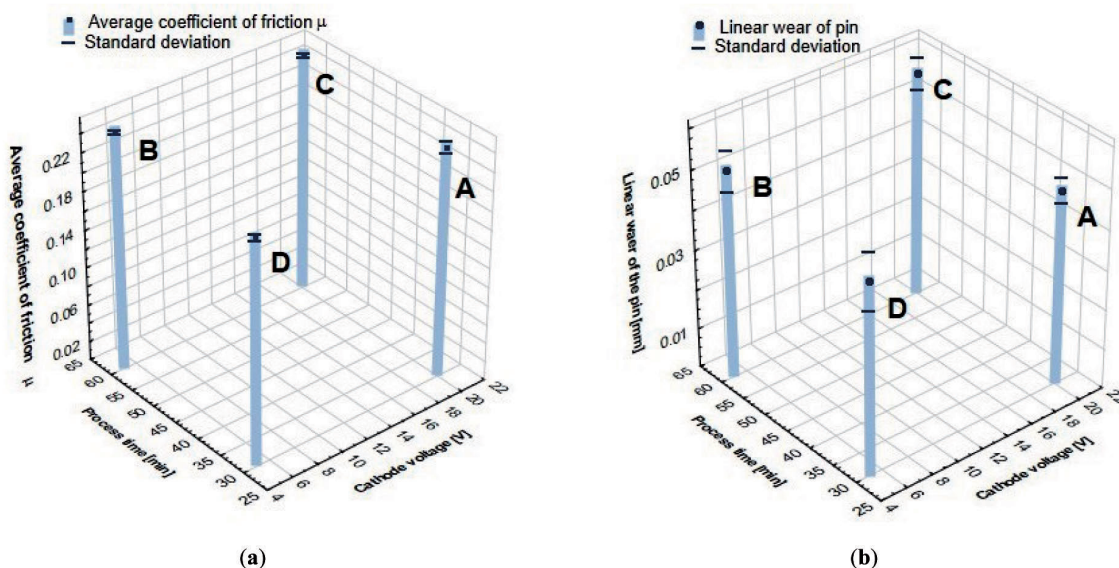


Fig. 2. Dependence of: (a) average value of coefficient of friction μ , (b) average linear wear of the pin; on the cathodic voltage and process time

Rys. 2. Zależność: (a) średniej wartości współczynnika tarcia μ , (b) średniego zużycia liniowego trzpienia od napięcia katodowania i czasu procesu

Table 4 shows the changes in the mass of the samples and the average mass wear of the PEEK-HPV pin cooperating with the AZ31B magnesium alloy and the oxide layers produced in the plasma electrolytic oxidation process. The highest mass loss was determined for the Mg sample (6.15 mg), which was not modified by plasma electrolytic oxidation, this sample was also characterized by the lowest wear of the plastic pin. Such parameters may indicate poor sliding cooperation between the sample and the counter-sample as a result of technically dry friction. The friction process results in a significant wear of the sample, with relatively

little wear of the polymer pin. For sample C, characterized by both the highest parameters of the plasma electrolytic oxidation process, thickness, coefficient of friction μ , and linear wear of the pin, the largest increase in sample weight (0.74 mg) was determined. A negative value of the mass wear of the sample proves that the sample wear is superior to the application of the sliding film, which has a negative effect on the sliding cooperation. Sample C was also characterized by the highest mass consumption of the pin (5.33 mg), which is related to the amount of film deposited on the surface of the layer.

Table 4. Mean values of sample mass change and mass wear of polymer pins

Tabela 4. Średnia zmiana masy próbki oraz zużycia masowego polimerowych trzpieni

Sample	Average Change in Sample Mass [mg]	Standard Deviation [mg]	Average Mass Wear of the Pin [mg]	Standard Deviation [mg]
A	0.4	0.05	4.57	0.04
B	0.53	0.04	4.9	0.04
C	0.74	0.04	5.33	0.04
D	0.35	0.06	4.03	0.05
Mg	-6.15	0.23	2.45	0.07

Figure 3 shows the dependence of the average change in the sample mass and the average wear of the polymer pin on the parameters of the production of oxide layers using graphs. The analysis of the dependence of the average change in the weight of the sample shows that most of the sliding film was applied to the layers produced within 60 minutes (samples B and C). The increase in the average weight change of the sample is greatly influenced by the increase in the cathodic voltage during the plasma electrolytic oxidation process, which is caused by the application of the sliding film. It can also be stated that the mass wear of the PEEK-HPV pin is directly proportional to the coefficient of friction μ and to the linear wear of the pin, where the increase in process time and cathodic voltage increases them.

Microscopic observation of the sliding films (**Figure 4**) allowed to analyze the application of the polymer on the surface of the samples

after sliding cooperation. On the figure show the mechanisms of tribological wear. The photos were taken in the middle of the slide track. The presented microscopic images show differences in the surface coverage of the samples with a polymer sliding film as a result of tribological cooperation. On sample C, characterized by the greatest wear of the pin during friction and the largest increase in sample weight, a significant amount of opaque sliding film is visible. The surface of sample D with the lowest wear of the pin and the smallest increase in mass is definitely less covered with a sliding film. The microscopic photos also show the different nature of the film application during the sliding cooperation with the magnesium alloy. The polymer film in this case is applied very unevenly along the friction path and is transparent. Combined with the significant consumption of the sample, this indicates poor sliding cooperation between the tribopartners.

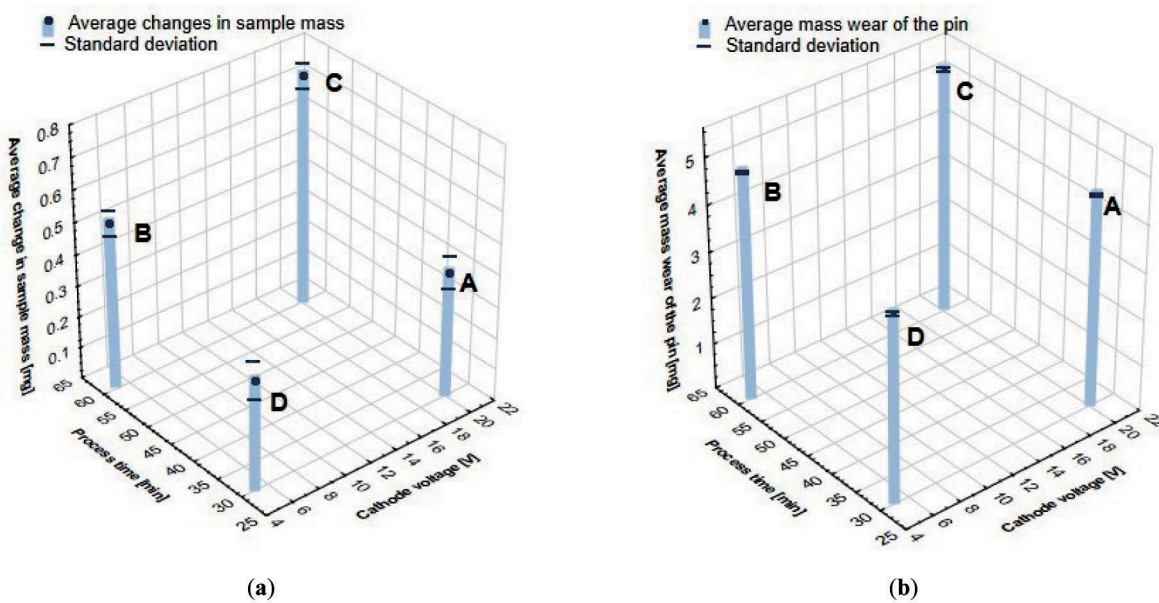


Fig. 3. Dependence of: (a) average change in sample mass, (b) average mass wear of the pin, on the cathodic voltage and process time

Rys. 3. Zależność: (a) średniej zmiany masy próbki, (b) średniego zużycia masowego trzpienia od napięcia katodowania i czasu procesu

Surface roughness is one of the most significant parameters in relation to tribological phenomena. The images of the surface roughness profiles of the samples before and after the tribological test (**Fig. 5**) allowed to present the differences in roughness resulting from the oxidation parameters (oxide layers) and changes as a result of technically dry friction. The oxide layers before the friction

process were characterized by differences in roughness, having a significant number of sharp peaks and depressions. The tribological test carried out on the oxide layers caused a significant smoothing of the sample surface by cutting off the tops and evenly applying the sliding film, partially filling the depressions. Before the tribological test, the surface of the magnesium alloy was

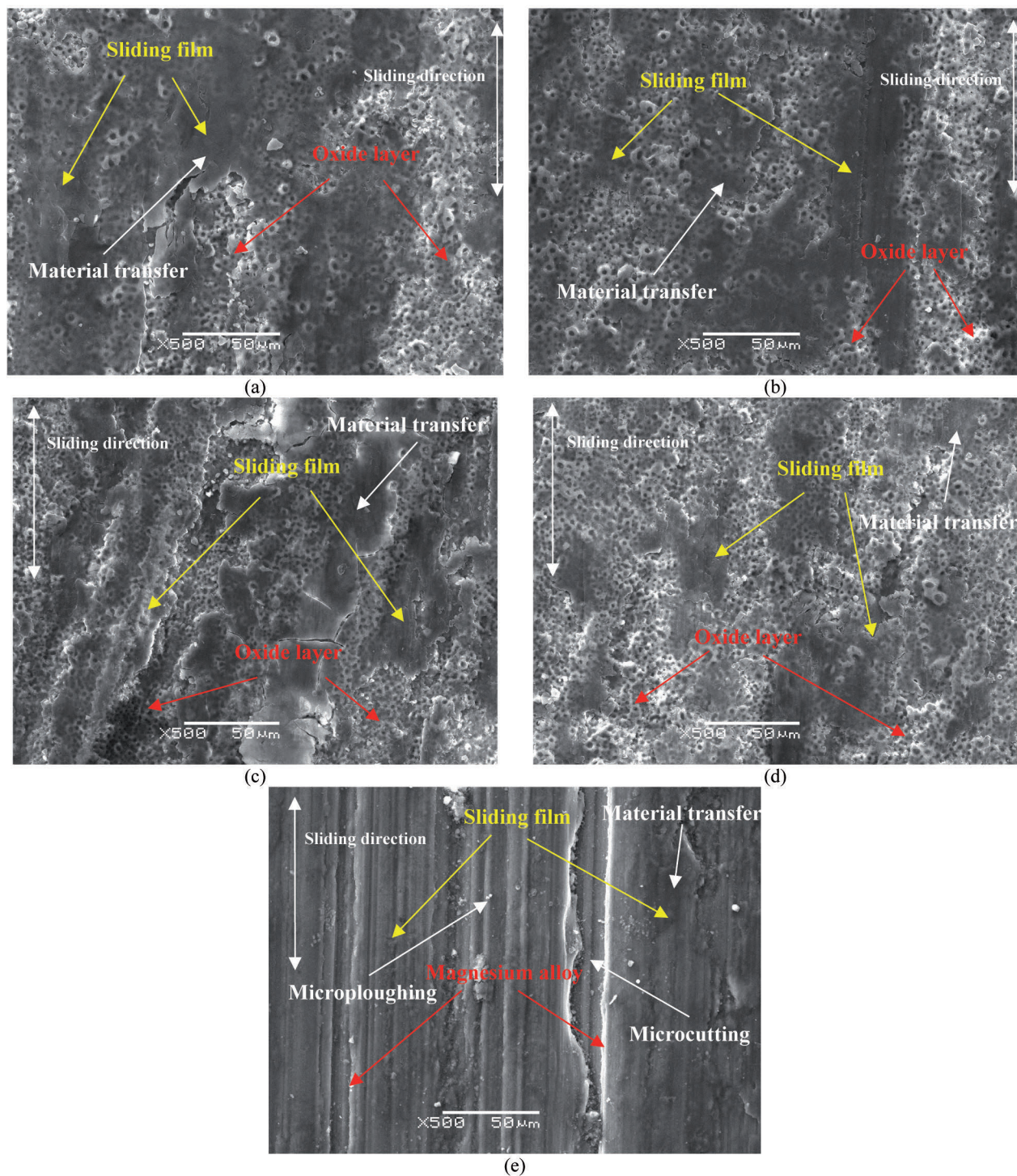


Fig. 4. Microscopic images of the surface after sliding cooperation for the sample: (a) A, (b) B, (c) C, (d) D, (e) Mg
 Rys. 4. Obrazy mikroskopowe powierzchni po współpracy ślizgowej dla próbek: (a) A, (b) B, (c) C, (d) D, (e) Mg

characterized by low roughness, but cooperation with the polymer caused a significant increase in roughness with the simultaneous appearance of many vertex peaks. This is the result of sample wear and a small amount of the sliding film applied during the friction process.

Table 5 presents the amplitude parameters that have the greatest impact on the sliding cooperation (R_q – mean square deviation of the profile from the mean line along the measurement or elementary section, R_{sk} – coefficient of skewness of the roughness profile, R_{ku} – coefficient of inclination

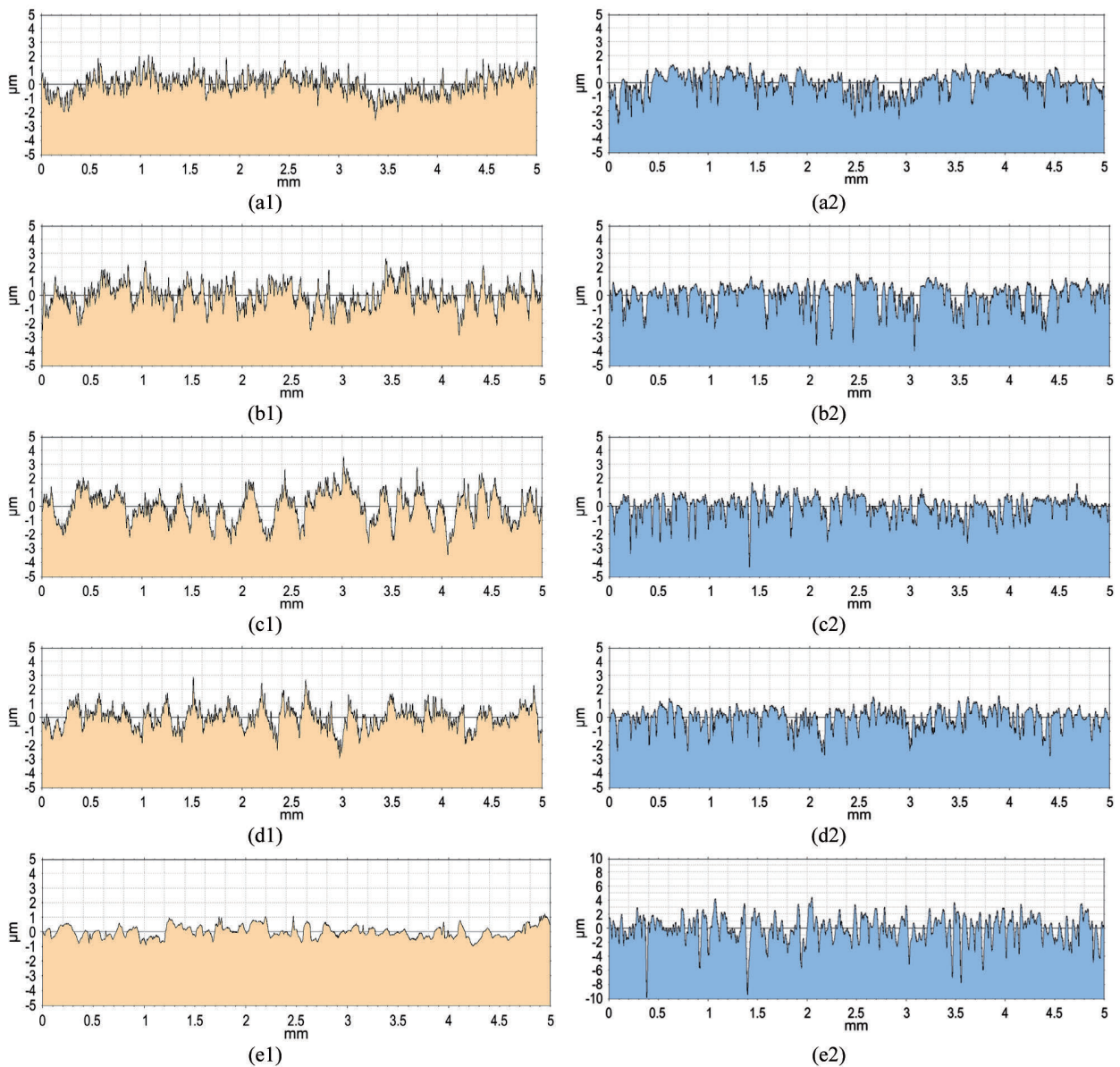


Fig. 5. Surface roughness profiles of oxide layers and magnesium alloy before (1) and after (2) tribological cooperation for the sample: a) A, b) B, c) C, d) D, e) Mg.

Rys. 5. Profile chropowości powierzchni warstw tlenkowych i stopu magnezu przed (1) i po (2) współpracy tribologicznej dla próbki: (a) A, (b) B, (c) C, (d) D, (e) Mg

of the roughness profile) before and after the tribological test. The analysis of the amplitude parameters before the tribological test shows visible changes resulting from the applied parameters for the production of layers and use of the alloy without modifications. Sample C was characterized by the highest R_q parameter, high R_{ku} parameter and the lowest R_{sk} parameter, which proves the bearing nature of the sample (negative value). In turn, the magnesium alloy had the lowest R_q parameter and the highest R_{ku} . The tribological cooperation influenced the change in the amplitude parameters

of the surface and for all samples with oxide layers the R_q parameter was reduced, but for the magnesium alloy it almost doubled. Such changes testify to the good cooperation of the applied material with the oxide layers and bad cooperation with the magnesium alloy. The R_{sk} parameter for all samples decreased and reached negative values, changing for samples A and D from the abrasive to the bearing nature of the cooperation. The R_{ku} parameter for all samples increased creating a more slender distribution.

Table 5. Mean values of amplitude parameters of sample surface roughness

Tabela 5. Średnie wartości parametrów amplitudowych chropowatości powierzchni próbek

Sample	Amplitude parameters					
	Rq [μm]	Standard Deviation [μm]	Rsk [μm]	Standard Deviation [μm]	Rku [μm]	Standard Deviation [μm]
Before test						
A	0.657	0.092	0.303	0.116	3.630	0.714
B	0.727	0.185	-0.310	0.111	3.447	0.345
C	0.982	0.219	-0.343	0.137	3.620	0.421
D	0.626	0.091	0.403	0.158	3.624	0.456
Mg	0.430	0.116	-0.022	0.087	3.953	0.489
After test						
A	0.548	0.051	-1.171	0.221	5.044	0.649
B	0.690	0.064	-1.316	0.138	5.185	0.417
C	0.711	0.084	-1.210	0.164	5.174	0.946
D	0.547	0.084	-1.155	0.179	4.767	1.025
Mg	2.01	0.139	-0.987	0.164	5.774	0.357

Table 6 presents the parameters of the load curve (Abbott-Firestone): Rk – depth of the roughness core, Rpk – reduced elevation height, Rvk – average depth of indentations before and after tribological tests. The highest values of these parameters were reached by sample C, also characterised by the highest coefficient of friction and the highest pin wear. This layer has a high Rvk parameter responsible for maintaining the sliding film on the surface of the layer, which is extremely important in the process of technically dry friction. The magnesium alloy before the tribological run

was characterized by low values of the load curve parameters. The tribological test for the oxide layers resulted in a reduction of the Rk and Rpk parameters, which means a significant smoothing of the sample by truncating the vertices and an increase in Rvk as a result of the unevenly applied sliding film. This means a significant smoothing of the sample by truncating the vertices. The magnesium alloy sample significantly increased the parameters of the load curve as a result of friction (up to six times), which is caused by significant and uneven wear during the test.

Table 6. Mean values of the layer surface bearing curve parameters

Tabela 6. Średnie wartości parametrów krzywej nośności powierzchni warstw

Sample	Parameters of the load curve (Abbott-Firestone)					
	Rk [μm]	Standard Deviation [μm]	Rpk [μm]	Standard Deviation [μm]	Rvk [μm]	Standard Deviation [μm]
Before test						
A	1.762	0.206	0.698	0.138	0.740	0.184
B	1.929	0.347	0.744	0.075	1.051	0.354
C	2.560	0.254	0.820	0.106	1.268	0.211
D	1.616	0.189	0.696	0.107	0.657	0.164
Mg	0.966	0.178	0.475	0.173	0.593	0.157
After test						
A	1.034	0.160	0.333	0.354	1.133	0.142
B	1.254	0.052	0.364	0.072	1.456	0.249
C	1.305	0.138	0.413	0.167	1.328	0.297
D	1.035	0.182	0.035	0.032	1.072	0.111
Mg	4.358	0.145	3.043	0.448	3.998	0.519

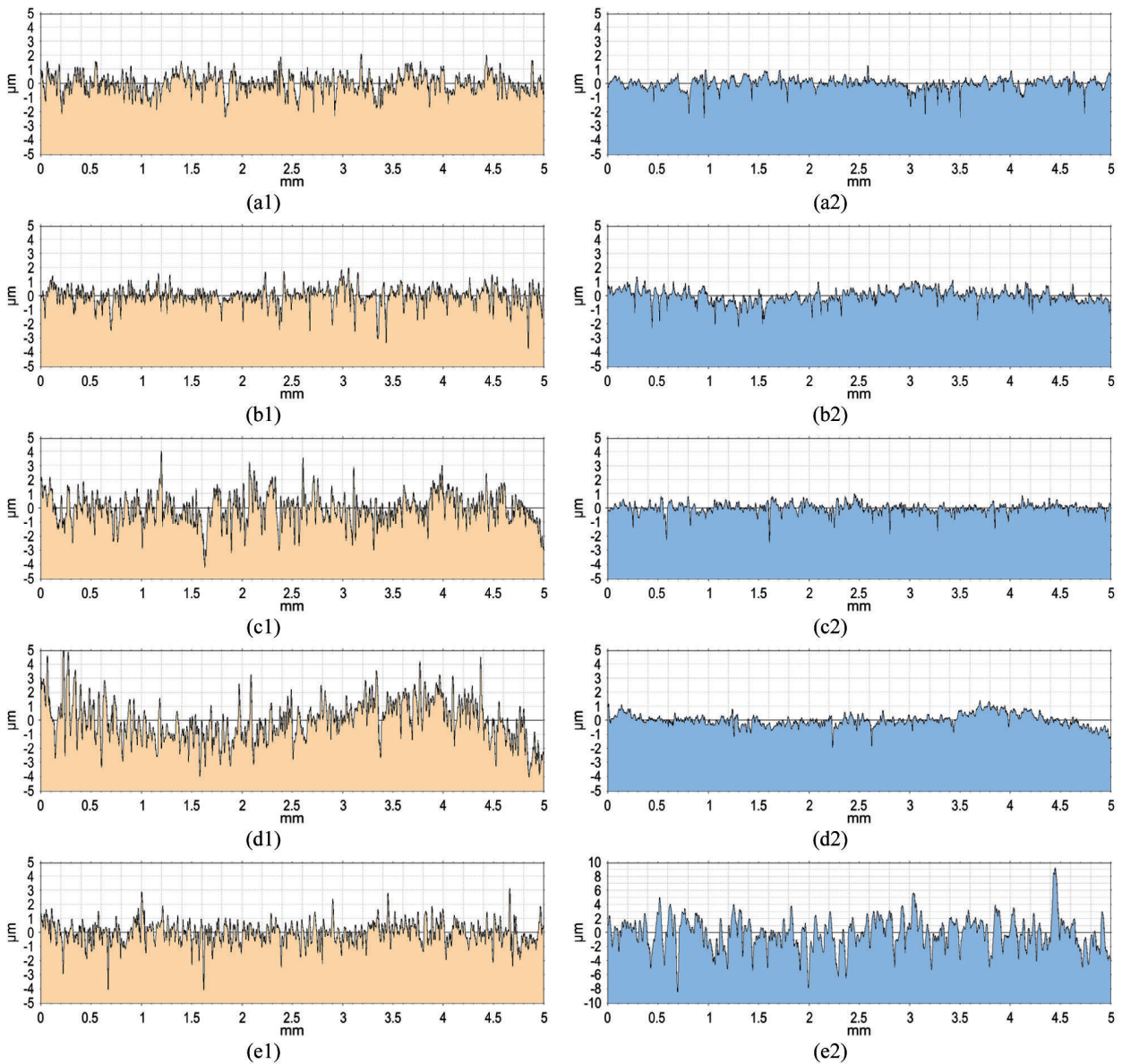


Fig. 6. Surface roughness profiles of the polymer pin before (1) and after (2) tribological cooperation for the sample: (a) A, (b) B, (c) C, (d) D, (e) Mg

Rys. 6. Profile chropowości powierzchni trzpienia polimerowego przed (1) i po (2) współpracy tribologicznej dla próbki: (a) A, (b) B, (c) C, (d) D, (e) Mg

The images of the roughness profiles for the pins (**Fig. 6**) made it possible to visualize the surface roughness of the material before and after the tribological test. The studs before the tribological run were characterized by similar roughness, slight differences result from their uneven grinding. Tribological tests contributed to a decrease in the roughness of the material (oxide layers) and a significant increase in roughness (magnesium alloy).

The roughness of the plastic pins constituting the tribopartner for the samples was determined

based on the measurement of the amplitude parameter R_q before and after the tribological test. Parameters R_q denoting the mean square deviation of the profile from the mean line along the measuring or elementary section are summarized in **Table 7**. Before the tribological test, all pins were prepared in the same way, by grinding on sandpaper, small differences in the R_q parameter before the tribological run testify to their similar roughness. The tribological test for all oxide layers contributed to the reduction of the pin roughness, which proves that the material wears evenly

and is deposited on the surface of the layer. This contributes to the change from layer-to-plastic to plastic-to-plastic cooperation. As a result of the tribological cooperation of the magnesium alloy with the plastic, the R_q parameter for the pin increased more than five times, which proves the uneven wear of the pin, combined with the wear of the sample surface and a slight deposition of the sliding film.

Table 7. Mean value of the R_q amplitude parameter of polymer pins

Tabela 7. Średnia wartość parametru amplitudowego R_q trzpieni polimerowych

Sample	R_q [μm]	Standard Deviation [μm]
Before test		
A	0.941	0.131
B	0.993	0.128
C	0.867	0.148
D	0.908	0.189
Mg	0.842	0.136
After test		
A	0.422	0.038
B	0.506	0.042
C	0.737	0.006
D	0.772	0.007
Mg	2.262	0.158

CONCLUSIONS

- The research presented in the article confirms the legitimacy of plasma electrolytic oxidation of the AZ31B magnesium alloy to improve tribological properties.
- Changing the oxidation parameters (cathodizing voltage and process time) influence changes in the thickness of the oxide layer. Both the increase in the cathodic voltage and the process time affect the increase in the layer thickness, contributing to the increase in the efficiency of the process (increased thickness with the same anode voltage), as well as the creation of a surface with greater roughness.
- Parameters of the oxidation process strongly affect the tribological parameters. It was found that the increase in both the process time and the cathodic voltage increased the coefficient of friction μ and the wear R of the polymer pin. The largest amounts of the polymer slip film were

deposited on the layers produced in 60 minutes. An increase in the average weight change of the sample was observed as a result of the increase in the cathodic voltage.

- SEM tests of the surface of the samples showed the deposition of a polymer sliding film on their surfaces. Sample C, characterized by the highest coefficient of friction μ and pin wear, has a significant amount of opaque sliding film. In turn, the cooperation of the material with the magnesium alloy (Mg sample) resulted in uneven deposition (along the friction path) of a transparent sliding film.
- Measurements of the surface amplitude parameters showed differences between successive layers, but also between the magnesium alloy. The highest surface roughness was characterized by sample C, which also, together with sample B and Mg, had a negative R_{sk} parameter, proving the bearing nature of the surface. The tribological cooperation influenced the smoothing of the surface of the oxide layers, shearing the tops and evenly applying a sliding film on the surface. The tribological cooperation of the polymer with the Mg sample contributed to a significant increase in its roughness, as a result of significant surface wear.
- The analysis of the load curve parameters showed differences in their values depending on the manufacturing parameters. The highest parameters of the load-bearing curve are characteristic of sample C, the layer of which was produced within 60 minutes at the cathodic voltage of 20 V. It has a high R_{vk} parameter, responsible for maintaining the sliding film on the surface of the layer. As a result of the tribological test of the oxide layers, R_k and R_{pk} parameters (surface smoothing) were reduced and R_{vk} increased. The Mg sample before the friction process had low parameters of the load curve. The tribological test for the Mg sample caused a significant increase in the parameters of the load curve as a result of its uneven wear and a small amount of sliding film.
- The measurement of amplitude parameter R_q for the plastic pins used during the test allowed a conclusion that their cooperation with the oxide layers was good (reduction of the R_q parameter) and bad with the magnesium alloy (definite increase of the R_q parameter). In the case of oxide layers, due to the application of a sliding film, the cooperation changes from metal-plastic to plastic-plastic.

REFERENCES

1. Castellanos, A., Altube, A., Vega, J.M., García-Lecina, E., Díez, J.A., Grande, H.J.: Effect of different post-treatments on the corrosion resistance and tribological properties of AZ91D magnesium alloy coated PEO. *Surf. Coat. Technol.* 278, 2015, pp. 99–107.
2. Anawati, A., Hidayati, E., Labibah, H.: Characteristics of magnesium phosphate coatings formed on AZ31 Mg alloy by plasma electrolytic oxidation with improved current efficiency. *Mater. Sci. Eng. B.* 272, 2021, pp. 1–10.
3. Liu, J.Z., Zhao, Y.H., Song, L., Xiang, Z.X.: Study on the AZ31B Magnesium Alloy in the Application on High-Speed Trains. *Adv. Mat. Res.* 535–537, 2012, pp. 875–879.
4. Darband, B.Gh., Aliofkhaezai, M., Hamghalam, P., Valizade, N.: Plasma electrolytic oxidation of magnesium and its alloys: Mechanism, properties and applications. *J. Magnes. Alloy.* 5, 2017, pp. 74–132.
5. Tu, X., Miao, Ch., Zhang Y., Li, J.: Plasma Electrolytic Oxidation of Magnesium Alloy AZ31B in Electrolyte Containing Al_2O_3 Sol as Additives. *Mater.* 11, 2018, pp. 1–11.
6. Niedźwiedź, M., Bara, M., Skoneczny, W., Kaptacz, S., Dercz, G.: Influence of Anodizing Parameters on Tribological Properties and Wettability of Al_2O_3 Layers Produced on the EN AW-5251 Aluminum Alloy. *Materials.* 15, 2022, pp. 1–21.
7. Joahri, N.A., Alias, J., Zanurin, A., Mohamed, N.S., Alang, N.A., Zain, M.Z.M.: Anti-corrosive coatings of magnesium: A review. *Mater. Today-Proc.* 48, 2022, pp. 1842–1848.
8. Verdier, S., Boinet, M., Maximovitch, S., Dalard, F.: Formation, structure and composition of anodic films on AM60 magnesium alloy obtained by DC plasma anodizing. *Corros. Sci.* 47, 2005, pp. 1429–1444.
9. Zhang, W., Du, Y., Zhang, P.: Excellent plasma electrolytic oxidation coating on AZ61 magnesium alloy under ordinal discharge mode. *J. Magnes. Alloy.* 10, 2022, pp. 2460–2474.
10. Pezzato, L., Lorenzetti, L., Tonelli, L., Bragaglia, G., Dabalà, M., Martini, C., Brunelli, K.: Effect of SiC and borosilicate glass particles on the corrosion and tribological behavior of AZ91D magnesium alloy after PEO process. *Surf. Coat. Technol.* 428, 2021, pp. 1–16.
11. Gray, X., Luan, B.: Protective coatings on magnesium and its alloys – A critical review. *J. Alloys Compd.* 336, 2002, pp. 88–113.
12. Chen, X., Birbilis, N., Abbott, T.: Review of corrosion-resistant conversion coatings for magnesium and its alloys. *Corrosion.* 67, 2011, pp. 1–16.
13. Song, G., Shi, Z.: Anodization and corrosion of magnesium (Mg) alloys. In *Corrosion Prevention of Magnesium Alloys*, Woodhead Publishing Limited, Oxford, UK, 2013.
14. Yerokhin, A.L., Nie, X., Leyland, A., Matthews, A., Dowey, S.J.: Plasma electrolysis for surface engineering. *Surf. Coat. Technol.* 122, 1999, pp. 73–93.
15. Guo, Y., Rogov, A., Hird, A., Mingo, B., Matthews, A., Yerokhin, A.: Plasma electrolytic oxidation of magnesium by sawtooth pulse current. *Surf. Coat. Technol.* 429, 2022, p. 127938.
16. Rogov, A.B., Matthews, A., Yerokhin, A.: Relaxation Kinetics of Plasma Electrolytic Oxidation Coated Al Electrode: Insight into the Role of Negative Current. *J. Phys. Chem. C.* 124, 2020, pp. 23784–23797.